14. Ericzon BG, Larsson M, Wilczek HE. Domino liver transplantation: risks and benefits. Transplant Proc 2008; 40: 1130-1131.

15. Barreiros AP, Post F, Hoppe-Lotichius M, Linke RP, Vahl CF, Schäfers HJ, et al. Liver transplantation and combined liver-heart transplantation in patients with familial amyloid polyneuropathy: A single-center experience. Liver Transpl 2010; 16: 314-323.

16. Lladó L, Baliellas C, Casasnovas C, Ferrer I, Fabregat J, Ramos E, et al. Risk of transmission of systemic transthyretin amyloidosis after domino liver transplantation. Liver Transpl 2010; 16: 1386-1392.

17. Conceição I, Evangelista T, Castro J, Pereira P, Silvestre A, Coutinho CA, et al. Acquired amyloid neuropathy in a Portuguese patient after domino liver transplantation. Muscle Nerve 2010; 42: 836-839.

18. Obayashi K, Yamashita T, Tasaki M, Ueda M, Shono M, Jono H, et al. Amyloid neuropathy in a younger domino liver transplanted recipient. Muscle Nerve 2011; 43: 449-450.

19. Koike H, Kiuchi T, Iijima M, Ueda M, Ando Y, Morozumi S, et al. Systemic but asymptomatic transthyretin amyloidosis 8 years after domino liver transplantation. J Neurol Neurosurg Psychiatry 2011; 82: 1287-1290.

20. Pradotto L, Franchello A, Milesi A, Romagnoli R, Bigoni M, Vigna L, et al. Amyloid polyneuropathy following domino liver transplantation. Muscle Nerve 2012; 45: 918-919.

21. Bolte FJ, Schmidt HH, Becker T, Braun F, Pascher A, Klempnauer J, et al. Evaluation of domino liver transplantations in Germany. Transpl Int 2013; 26: 715-723.

22. Abdelfatah MM, Hayman SR, Gertz MA. Domino liver transplantation as a cause of acquired familial amyloid polyneuropathy. Amyloid 2014; 21: 136-137.

23. Tashima K, Ando Y, Terazaki H, Yoshimatsu S, Suhr OB, Obayashi K, et al. Outcome of liver transplantation for transthyretin amyloidosis: follow-up of Japanese familial amyloidotic polyneuropathy patients. J Neurol Sci 1999; 171: 19-23.

24. Jack CR Jr, Wiste HJ, Weigand SD, Rocca WA, Knopman DS, Mielke MM, et al. Age-specific population frequencies of cerebral β-amyloidosis and neurodegeneration among people with normal cognitive function aged 50-89 years: A cross-sectional study. Lancet Neurol 2014; 13: 997-1005.

25. Solomon A, Murphy CL, Kestler D, Coriu D, Weiss DT, Makovitzky J, et al. Amyloid contained in the knee joint meniscus is formed from apolipoprotein A-I. Arthritis Rheum 2006; 54: 3545-3550.

26. Su Y, Misumi Y, Ueda M, Shono M, Tasaki M, Guo J, et al. The occurrence of islet amyloid polypeptide amyloidosis in Japanese subjects. Pancreas 2012; 41: 971-973.

27. Okuda Y, Yamada T, Matsuura M, Takasugi K, Goto M. Ageing: A risk factor for amyloid A amyloidosis in rheumatoid arthritis. Amyloid 2011; 18: 108-111.

28. Koike H, Kawagashira Y, Iijima M, Yamamoto M, Hattori N, Tanaka F, et al. Electrophysiological features of late-onset transthyretin Met30 familial amyloid polyneuropathy unrelated to endemic foci. J Neurol 2008; 255: 1526-1533.

29. Takahashi R, Ono K, Shibata S, Nakamura K, Komatsu J, Ikeda Y, et al. Efficacy of diflunisal on autonomic dysfunction of late-onset familial amyloid polyneuropathy (TTR Val30Met) in a Japanese endemic area. J Neurol Sci 2014; 345: 231-235.

30. Sueyoshi T, Ueda M, Jono H, Irie H, Sei A, Ide J, et al. Wild-type transthyretin-derived amyloidosis in various ligaments and tendons. Hum Pathol 2011; 42: 1259-1264.

31. Yanagisawa A, Ueda M, Sueyoshi T, Okada T, Fujimoto T, Ogi Y, et al. Amyloid deposits derived from transthyretin in the ligamentum flavum as related to lumbar spinal canal stenosis. Mod Pathol 2015; 28: 201-207.

32. Buxbaum J, Koziol J, Connors LH. Serum transthyretin levels in senile systemic amyloidosis: Effects of age, gender and ethnicity. Amyloid 2008; 15: 255-261.

33. Hurshman AR, White JT, Powers ET, Kelly JW. Transthyretin aggregation under partially denaturing conditions is a downhill polymerization. Biochemistry 2004; 43: 7365-7381.

34. Bateman RJ, Xiong C, Benzinger TL, Fagan AM, Goate A, Fox NC, et al. Clinical and biomarker changes in dominantly inherited Alzheimer's disease. N Engl J Med 2012; 367: 795-804.

Figure legends

Figure 1: *De novo* amyloid deposition and symptoms of DLT recipients

Kaplan-Meier curves for the estimated occurrence of *de novo* amyloid deposition (solid lines) and symptoms of amyloidosis (dashed lines) after DLT in recipients of domino liver grafts obtained from hereditary TTR amyloidosis patients with (A) all DLT recipients, (B) V30M (p. V50M), and (C) non-V30M. DLT, domino liver transplantation.

Figure 2: Relationship between clinical characteristics of DLT donors (hereditary TTR amyloidosis patients) and *de novo* amyloid deposition in DLT recipients

(A) Kaplan-Meier curve for the estimated occurrence of *de novo* amyloid deposition in recipients of livers explanted from male (dashed line) and female (solid line) domino liver donors. (B) Relationship between degrees of amyloid deposition (none, mild: not circumferential, or severe: circumferential deposition) in explanted livers and *de novo* amyloid deposition in domino liver recipients.

The plot shows the time from the DLT to the first detection of amyloid in patients with amyloid deposition (filled circles) and the observation time from the DLT in patients without amyloid deposition (open circles). DLT, domino liver transplantation.

Figure 3: Relationship between clinical characteristics of DLT recipients and *de novo*

amyloid deposition

(A) Kaplan-Meier curve for the estimated occurrence of *de novo* amyloid deposition in male (dashed line) and female (solid line) domino liver recipients. (B) Kaplan-Meier curve for the estimated occurrence of *de novo* amyloid deposition in older liver recipients (more than 50 years old at the time of DLT: solid line) and younger liver re

cipients (less than 50 years old at the time of DLT: dashed line). (C) Relationship between the age of domino liver recipients at the time of DLT and the time to first detection of amyloid deposition. R = 0.80, p = 0.048. (D) Semiquantitative analysis of Congo red positive areas in the subcutaneous fat tissue in the domino recipients (filled circles: more than 50 years old, open circles: less than 50 years old at the time of DLT). (E) Congo red-stained section of a gastric mucosal biopsy from a 63-year-old recipient at 5 years after DLT. BF, bright-field; PL, polarized light. Scale bar = 50 μm.

DLT, domino liver transplantation.

Table 1: Clinical profiles of domino liver donors and recipients

Case	Donors			Recipients (patients with hereditary TTR amyloidosis)						
	Age at LT (years)	Sex	TTR mutation	Age at LT (years)	Sex	Primary disease	Immunosuppressants	Observation period (months)	Amyloid deposition	Alive or dead
1	58	M	V30M	50	F	PBC	Tac	95	+	Alive
2	29	M	V30M	35	M	LC	Tac, MMF	175	+	Alive
3	49	M	V30M	41	M	PSC	Tac, MMF	162	-	Alive
4	39	M	Y114C	30	M	LC	Tac	96	+	Dead (metastasis)
5	50	M	S50I	60	M	HBV, LC	Tac	132	+	Alive
6	32	M	V30M	52	F	PBC	Tac, MMF, Pred	129	-	Alive
7	40	F	V30M	53	F	HBV, LC	Tac, MMF	91	+	Dead (metastasis)
8	28	M	V30M	35	F	BA	Tac	123	+	Alive
9	42	F	V30M	40	M	HCV, LC, HCC	Tac	15	-	Dead (metastasis)
10	27	F	V30M	23	F	BA	Tac	102	-	Alive
11	31	F	V30M	57	M	HCV, LC, HCC	Tac	26	-	Dead (metastasis)
12	31	F	V30M	18	M	BA	Tac, MMF, Pred	106	+	Alive
13	39	F	V30M	58	M	LC	Tac	72	+	Alive
14	36	F	V30M	43	M	HCV, LC	Tac, MMF, Pred	65	-	Alive
15	29	M	V30M	56	M	LC, HCC	Tac, MMF	66	-	Alive
16	51	F	V30M	58	M	HCV, LC, HCC	Tac, MMF	63	-	Alive
17	33	F	V30M	54	M	HBV, LC	Tac, MMF	49	-	Alive
18	44	F	V30M	35	M	PBC	Tac, MMF, Pred	5	-	Dead (liver failure)
19	41	M	V30M	45	F	LC	Tac	6	-	Dead (liver failure)
20	30	M	L55P	53	M	HCV, LC, HCC	Tac, MMF	10	-	Alive
21	27	F	V30M	62	M	HCV, LC	Tac, MMF	7	-	Alive
22	29	F	V30M	59	M	HBV, LC, HCC	Tac, MMF	6	-	Alive

BA, biliary atresia; HBV, hepatitis B virus infection; HCC, hepatocellular carcinoma; HCV, hepatitis C virus infection; LC, liver cirrhosis; LT, liver transplantation; MMF, mycophenolate mofetil; PBC, primary biliary cirrhosis; Pred, prednisolone; PSC, primary sclerosing cholangitis; Tac, tacrolimus; TTR, transthyretin.

Table 2: Symptoms in domino liver transplant recipients with amyloid deposition

Case	Polyneuropathy	Gastrointestinal symptoms	Arrhythmia	Heart failure	Vitreous opacity
1	+	-	-	-	-
2	+	+	-	-	-
4	-	-	-	-	-
5	+	-	-	-	-
7	-	-	-	-	-
8	+	-	-	-	-
12	-	-	-	-	-
13	+	+	-	-	-

Table 3: Sex, age, disease duration, and FAP clinical score of domino liver donors (hereditary TTR amyloidosis patients) at LT

Characteristics of donors	Recipients with amyloid	Recipients without amyloid	p-Value
Sex	50.0% male	31.0% male	
Age (years, mean ± SD)	37.5 ± 10.3	36.2 ± 8.0	0.41
Disease duration (years, mean ± SD)	2.2 ± 1.6	2.3 ± 1.4	0.48
FAP clinical score	9.0 ± 5.5	14.0 ± 10.0	0.10

FAP, familial amyloid polyneuropathy; LT, liver transplantation; SD, standard deviation.

Supplemental Table 1: Follow-up examinations interval for domino liver recipients

	Recipients with amyloid (times/ year)	Recipients without amyloid (times/ year)
Neurological examination	1.3 ± 0.7	1.3 ± 0.4
Nerve conduction study	0.2 ± 0.2	0.3 ± 0.5
Histopathological examination	0.7 ± 0.4	0.8 ± 0.7

Figure 1

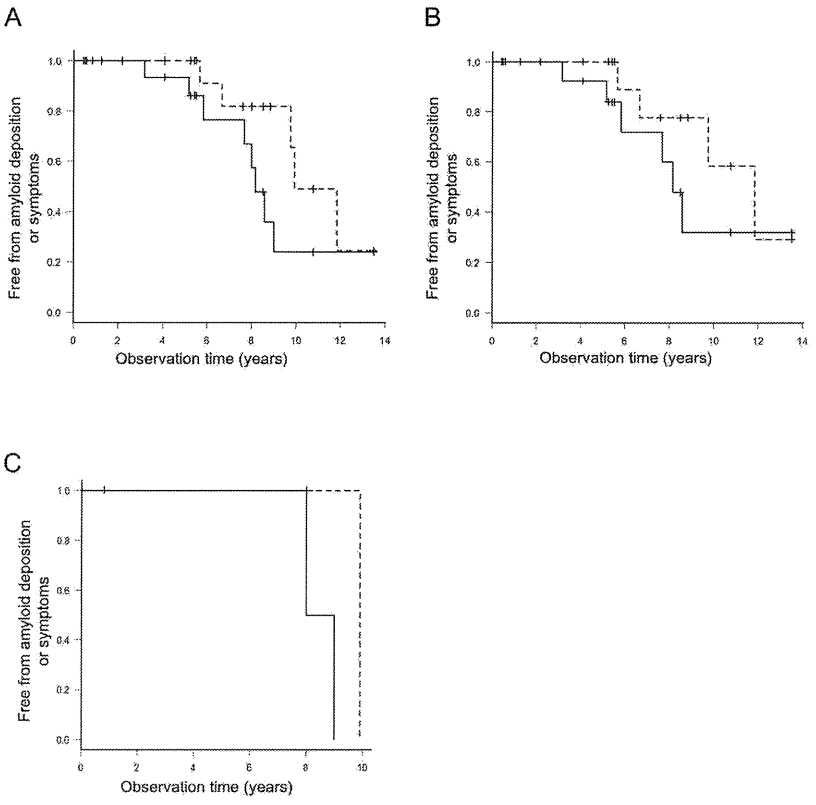

Figure 1: De novo amyloid deposition and symptoms of DLT recipients
Kaplan-Meier curves for the estimated occurrence of de novo amyloid deposition (solid lines) and symptoms of amyloidosis (dashed lines) after DLT in recipients of domino liver grafts obtained from hereditary TTR amyloidosis patients with (A) all DLT recipients, (B) V30M (p. V50M), and (C) non-V30M. DLT, domino liver transplantation.
209x294mm (300 x 300 DPI)

Figure 2

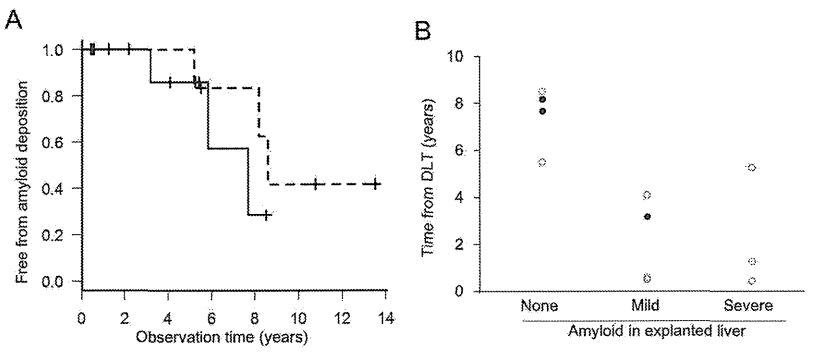

Figure 2: Relationship between clinical characteristics of DLT donors (hereditary TTR amyloidosis patients) and de novo amyloid deposition in DLT recipients
(A) Kaplan-Meier curve for the estimated occurrence of de novo amyloid deposition in recipients of livers explanted from male (dashed line) and female (solid line) domino liver donors. (B) Relationship between degrees of amyloid deposition (none, mild: not circumferential, or severe: circumferential deposition) in explanted livers and de novo amyloid deposition in domino liver recipients.
The plot shows the time from the DLT to the first detection of amyloid in patients with amyloid deposition (filled circles) and the observation time from the DLT in patients without amyloid deposition (open circles).
DLT, domino liver transplantation.
209x294mm (300 x 300 DPI)

Figure 3

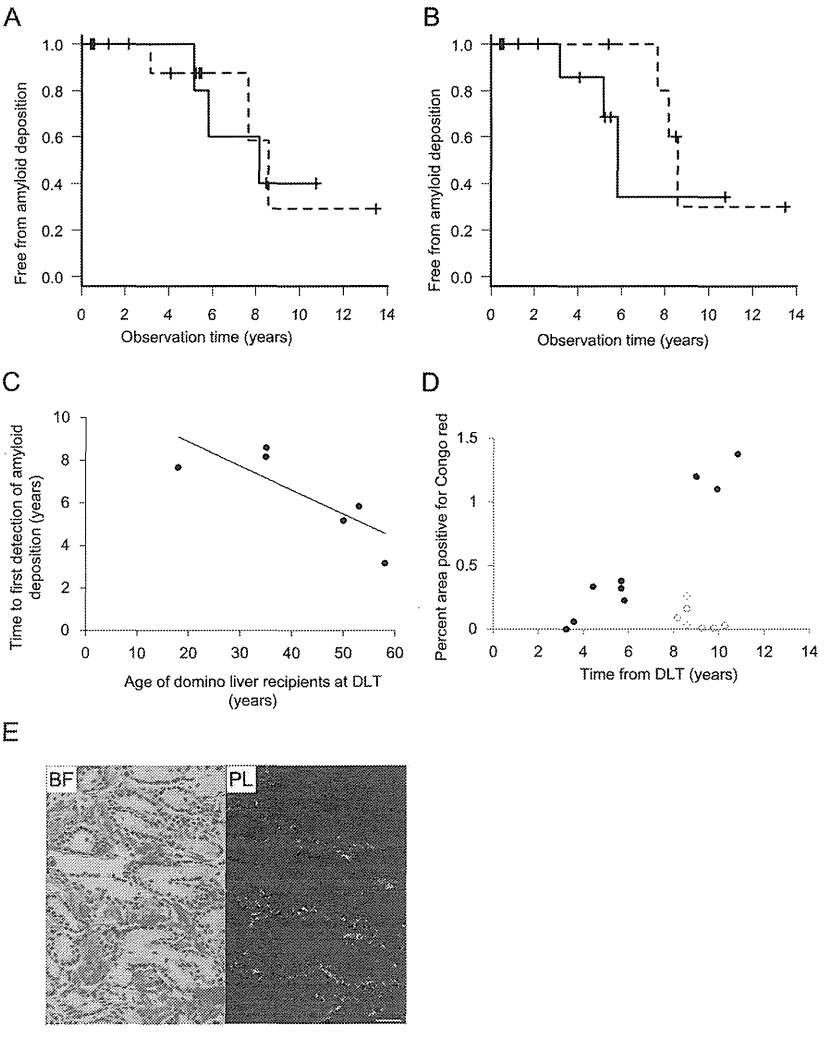

Figure 3: Relationship between clinical characteristics of DLT recipients and de novo amyloid deposition (A) Kaplan-Meier curve for the estimated occurrence of de novo amyloid deposition in male (dashed line) and female (solid line) domino liver recipients. (B) Kaplan-Meier curve for the estimated occurrence of de novo amyloid deposition in older liver recipients (more than 50 years old at the time of DLT: solid line) and younger liver re
cipients (less than 50 years old at the time of DLT: dashed line). (C) Relationship between the age of domino liver recipients at the time of DLT and the time to first detection of amyloid deposition. R = 0.80, p = 0.048. (D) Semiquantitative analysis of Congo red positive areas in the subcutaneous fat tissue in the domino recipients (filled circles: more than 50 years old, open circles: less than 50 years old at the time of DLT). (E) Congo red-stained section of a gastric mucosal biopsy from a 63-year-old recipient at 5 years after DLT. BF, bright-field; PL, polarized light. Scale bar = 50 μm.
DLT, domino liver transplantation.

Amyloid
The Journal of Protein Folding Disorders

http://informahealthcare.com/amy
ISSN: 1350-6129 (print), 1744-2818 (electronic)

Amyloid, 2015; 22(3): 181–186
 DOI: 10.3109/13506129.2015.1064818

informa
healthcare

ORIGINAL ARTICLE

Inhibition of insulin amyloid fibril formation by cyclodextrins

Keisuke Kitagawa[1]*, Yohei Misumi[1]*, Mitsuharu Ueda[1], Yuya Hayashi[2], Masayoshi Tasaki[1], Konen Obayashi[3], Taro Yamashita[1], Hirofumi Jono[4], Hidetoshi Arima[2], and Yukio Ando[1]

[1]*Department of Neurology, Graduate School of Medical Sciences, Kumamoto University, Kumamoto, Japan,* [2]*Department of Physical Pharmaceutics, Graduate School of Pharmaceutical Sciences, Kumamoto University, Kumamoto, Japan,* [3]*Department of Morphological and Physiological Sciences, Graduate School of Health Sciences, Kumamoto University, Kumamoto, Japan, and* [4]*Department of Clinical Pharmaceutical Sciences, Graduate School of Pharmaceutical Sciences, Kumamoto University, Kumamoto, Japan*

Abstract

Localized insulin-derived amyloid masses occasionally form at the site of repeated insulin injections in patients with insulin-dependent diabetes and cause subcutaneous insulin resistance. Various kinds of insulin including porcine insulin, human insulin, and insulin analogues reportedly formed amyloid fibrils *in vitro* and *in vivo*, but the impact of the amino acid replacement in insulin molecules on amyloidogenicity is largely unknown. In the present study, we demonstrated the difference in amyloid fibril formation kinetics of human insulin and insulin analogues, which suggests an important role of the C-terminal domain of the insulin B chain in nuclear formation of amyloid fibrils. Furthermore, we determined that cyclodextrins, which are widely used as drug carriers in the pharmaceutical field, had an inhibitory effect on the nuclear formation of insulin amyloid fibrils. These findings have significant implications for the mechanism underlying insulin amyloid fibril formation and for developing optimal additives to prevent this subcutaneous adverse effect.

Keywords

Amyloid, cyclodextrins, insulin, insulin analogue, insulin ball

History

Received 31 January 2015
Revised 29 May 2015
Accepted 18 June 2015
Published online 23 July 2015

Abbreviations: CyDs, cyclodextrins; GUG-β-CyD, 6-*O*-α-(4-*O*-α-D-glucuronyl)-D-glucosyl-β-CyD; HP-β-CyD, hydroxypropyl-β-CyD; ThT, thioflavin T.

Introduction

Amyloidosis comprises a group of diseases characterized by extracellular deposition of insoluble fibrillar proteins in localized or systemic organs. As of today, at least 31 different proteins have been determined to cause amyloidosis; these proteins include amyloidogenic immunoglobulin light chain, transthyretin, serum amyloid A, amyloid β, islet amyloid polypeptide, and insulin [1]. Amyloid fibrils induced by different precursor proteins have common structural and biochemical features: they are non-branching fibrils with diameters of approximately 10 nm, they manifest apple–green birefringence when stained with Congo red and visualized under polarized light, and they have a cross-β X-ray pattern [1]. Local insulin-derived amyloid masses (so-called insulin balls) have occasionally formed at sites of repeated insulin injections in patients with insulin-dependent diabetes [2–9]. Furthermore, severe subcutaneous insulin resistance in patients with blocked absorption of injected insulin was reportedly associated with insulin amyloidosis [10].

Insulin is a 51-residue peptide hormone and consists of primarily an α-helical A chain (21 residues) and a B chain (30 residues) linked by two disulfide bridges [11]. Previous *in vitro* investigations suggested that the insulin molecule underwent structural changes during the formation of amyloid fibrils, from a predominant α-helix to a β-sheet-rich conformation [12,13]. Elevated concentrations, high temperatures, greater ionic strength of the solution, and low pH all promoted formation of amyloid, as did preformed amyloid "seeds" [14]. The kinetics of insulin amyloid fibril formation showed a nucleation-dependent polymerization with a long lag phase during which no detectable amyloid fibrils formed, followed by an elongation phase [15]. Because early reported patients with insulin amyloidosis had been treated with non-human insulins, the non-human insulins were suspected of being the primary cause of amyloid fibril formation [6]. Human insulin and human insulin analogues were thereafter reported to form amyloid *in vitro* and *in vivo* [10]. However, the impact of the amino acid substitution in insulin molecules on amyloidogenicity is largely unknown. In this study, we therefore investigated the kinetics of amyloid fibril formation induced by human insulin and different types of insulin analogues.

*These authors contributed equally to this work.

Address for correspondence: Yohei Misumi, MD, PhD, Department of Neurology, Graduate School of Medical Sciences, Kumamoto University, 1-1-1 Honjo, Kumamoto 860-8556, Japan. Tel: +81-96-373-5893. Fax: +81 96 373 5895. E-mail: misumiyohei@hotmail.co.jp

Cyclodextrins (CyDs) are cyclic oligosaccharides that have a lipophilic central cavity and hydrophilic outer surface, and exhibit stability at high temperatures and extreme pH conditions. Because this structure serves as an inclusion site for hydrophobic molecules, CyDs are widely used as drug carriers in the pharmaceutical field [16]. Previous studies revealed that CyDs inhibited aggregation of pathogenic proteins including Aβ protein, α-synuclein [17], and transthyretin [18]. Certain studies revealed that β-CyD sulfate, sulfobutylether β-CyD, and maltosyl-β-CyD increased solubility and prevented self-association of insulin analogues *in vitro* and that they increased the bioavailability of insulin and persistence of the blood glucose-lowering effect *in vivo* [19,20]. However, the effects of CyDs on insulin amyloid fibril formation remain largely unknown. In this study, we analyzed the effect of CyDs on formation of amyloid fibrils derived from human insulin and different insulin analogues.

Materials and methods

Preparation of human insulin and insulin analogues

We used a recombinant human insulin (Humulin R®; Eli Lilly Japan, Kobe, Japan) and two insulin analogues, insulin aspart (NovoRapid®; Novo Nordisk Pharma, Tokyo, Japan) and insulin detemir (Levemir®; Novo Nordisk Pharma). To remove formulation buffers and excipients, human insulin and insulin analogues were dialyzed with 50-mM glycine buffer at pH 3.0 with a dialysis membrane (Spectra/Por MWCO 3500; Spectrum Laboratories, Rancho Dominguez, CA). Reaction solutions of dialyzed human insulin and insulin analogues were prepared immediately before the fibril formation process.

Insulin amyloid fibril formation

Insulin has a predominantly α-helical structure, and it has been shown that insulin forms amyloid fibrils under specific conditions such as low pH and high temperature [14]. Therefore, we performed *in vitro* experiment as follows. Reaction solutions included 200 μg/ml protein in 50-mM glycine-HCl buffer at pH 3.0, and they were incubated in Eppendorf tubes (1.5 ml) at 65 °C without agitation. To test the effect of preformed amyloid nuclei, reaction solutions that had been pre-incubated for 30 h were used as amyloid seeds. These seed solutions were added to freshly prepared reaction solutions to make 1% of total solution volume. All experiments were performed in triplicate.

Preparation of CyDs

HP-β-CyD (hydroxypropyl-β-CyD; Nihon Shokuhin Kako Co., Tokyo, Japan) and GUG-β-CyD [6-*O*-α-(4-*O*-α-D-glucuronyl)-D-glucosyl-β-CyD; Ensuiko Sugar Refining Co., Tokyo, Japan] were diluted in 50-mM glycine-HCl buffer at pH 3.0 immediately before the experiments.

All chemicals used in these studies were of analytical grade.

Thioflavin T (ThT) fluorescence measurement

We mixed 3 μl of reaction solution with 600 μl of thioflavin T (ThT) solution (5 μM in glycine-NaOH buffer at pH 9.5) in a glass cuvette. Fluorescence intensity was measured with a spectrofluorometer (F-2700; Hitachi, Tokyo, Japan) under the excitation and emission wavelengths of 444 and 482 nm, respectively. Each measurement was done in triplicate.

Transmission electron microscopy

A 3-μl aliquot of incubated sample was placed on a formvar-coated grid and allowed to adhere for 1 min, after which it was drained by using a strip of filter paper. The sample was then stained with a drop of 0.2% uranyl acetate for 1 min. After the excess stain was drained, the grid was air-dried and viewed with an electron microscope (H-7500; Hitachi High Technologies, Tokyo, Japan) at an accelerating voltage of 100 kV.

Results

Kinetics of amyloid fibril formation of human insulin and insulin analogues

Fibrillation of human insulin, the rapidly acting insulin analogue aspart, and the long-acting insulin analogue detemir was monitored as a function of time by measuring ThT fluorescence intensity and by using transmission electron microscopy. After incubation of insulin solutions at pH 3.0 and 65 °C, ThT fluorescence intensities followed a characteristic sigmoid curve, with an initial lag phase, an elongation phase, and a saturation phase. A shorter lag phase for insulin detemir and a much longer lag phase for insulin aspart were observed compared with the lag phase for human insulin (Figure 1A). Each solution showed similar ThT fluorescence intensities at the saturation phase. Human insulin and insulin analogues at the saturation phase produced showed typical needle-like amyloid fibrils of about 15 nm in diameter and several micrometers in length. The morphology of amyloid fibrils derived from human insulin and of the two insulin analogues did not differ significantly (Figure 1B). These kinetic profiles and morphological findings in amyloid fibril formation indicated a common nucleation-dependent polymerization mechanism but different lag-phase durations for human insulin and these two insulin analogues.

Effects of preformed amyloid seeds on insulin amyloid fibril formation

Because the major difference in amyloid fibril formation kinetics for human insulin, insulin aspart, and insulin detemir was the lag-phase duration, and the lag time is directly related to the formation of the amyloid nucleus, we expected that we could predict differences in the nuclear formation rate of insulin and insulin analogues. To confirm this expectation, we next tested the effects of preformed amyloid seeds on fibril formation. Seeding has reduced or even eliminated the lag phase for several types of amyloid precursor proteins including β_2-microglobulin, amyloid β, AA protein, and insulin [21].

With 1% of preformed amyloid seeds, the longest lag phase for insulin aspart was significantly shortened (Figure 2A), and the differences in lag-phase duration for human insulin, insulin aspart, and insulin detemir were reduced, which verified our hypothesis (Figure 2B, compare with Figure 1A).

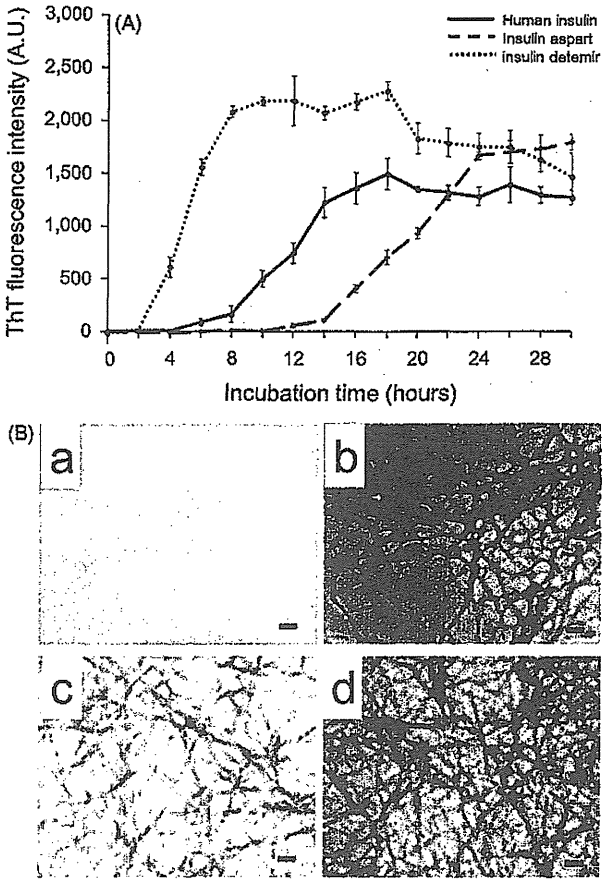

Figure 1. Kinetics of amyloid fibril formation of human insulin and insulin analogues. A, The time course of formation of amyloid fibrils was followed by measuring ThT fluorescence intensity. Human insulin (solid line), insulin aspart (dashed line), and insulin detemir (dotted line) were incubated at pH 3.0. Fluorescence intensity was measured at an excitation wavelength of 444 nm and an emission wavelength of 489 nm. A.U., arbitrary unit. B, Electron micrographs of human insulin (a) without and (b) with incubation; (c) insulin aspart with incubation; and (d) insulin detemir with incubation. Scale bars, 100 nm.

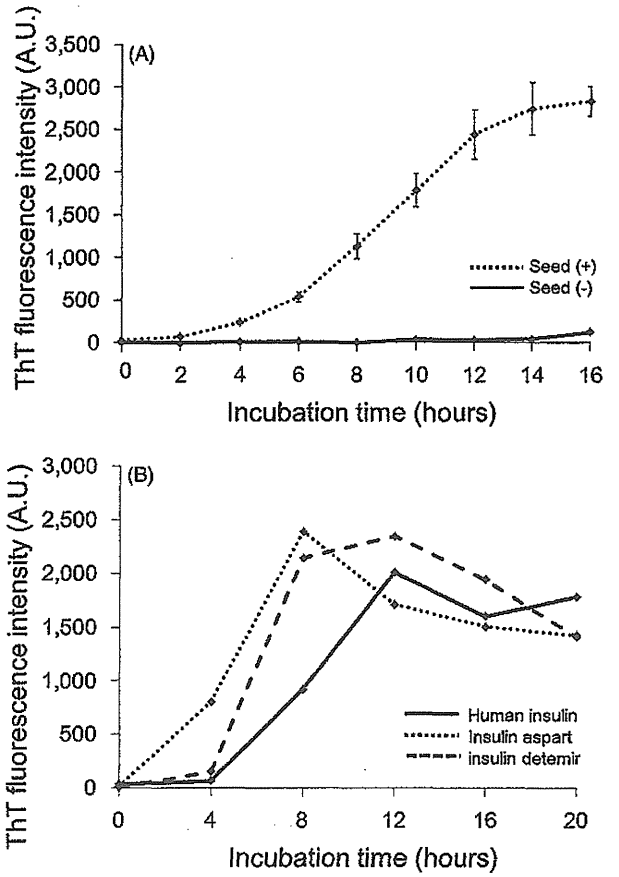

Figure 2. Effects of amyloid seeds on insulin amyloid fibril formation. A, Kinetics of amyloid fibril formation of insulin aspart with (dotted line) and without (solid line) 1% of preformed amyloid seeds. B, The time course of formation of amyloid fibrils derived from human insulin (solid line), insulin aspart (dotted line), and insulin detemir (dashed line) with 1% of preformed amyloid seeds. A.U., arbitrary unit.

Effects of CyDs on insulin amyloid fibril formation

To investigate whether the presence of HP-β-CyD or GUG-β-CyD had an effect on insulin fibril formation *in vitro*, we used the ThT fluorescence assay to measure the time course of reactions of insulin and insulin analogues with and without these CyDs. Both HP-β-CyD and GUG-β-CyD inhibited the amyloid fibril formation of human insulin and insulin analogues, but the degree of inhibition differed for each type of insulin (Figure 3A). HP-β-CyD inhibited insulin detemir with a greater efficiency compared with GUG-β-CyD. GUG-β-CyD, however, had a greater effect on insulin aspart. Both CyDs produced a small effect on human insulin amyloid fibril formation. Concentration-dependent inhibitory effects of GUG-β-CyD and HP-β-CyD on amyloid fibril formation of insulin detemir were confirmed (Figure 3B). The longer lag-phase duration with CyDs and the insulin analogues indicated that CyDs delayed the nuclear formation of amyloid fibrils. With 1% of preformed amyloid seeds, the effect of CyDs on the lag-phase duration on insulin aspart disappeared, as expected (Figure 3C).

Discussion

In the present study, we demonstrated differences in the rate of amyloid nuclear formation for human insulin and insulin analogues and an inhibitory effect of HP-β-CyD and GUG-β-CyD on this nuclear formation.

Insulin exists *in vivo* mainly as a homohexamer in the presence of the zinc ion. The mechanism of insulin amyloid fibrillation is hypothesized as follows: (1) dissociation of the native homohexamer into monomers, (2) misfolding of the monomeric insulin, (3) aggregation to form a nucleus, and (4) assembly into amyloid fibrils. In most insulin analogues, the C-terminus of the B chain is genetically modified to alter the stability of insulin dimers and hexamer, which achieves different durations of activity after injection. Hexamer stability is extremely low in the fast-acting insulin aspart and is high in the long-acting insulin detemir. One interesting finding was an accelerated nuclear formation of insulin detemir and a slowed nuclear formation of insulin aspart, as Figure 1 shows; nuclear formation is thus the rate-limiting step of amyloid fibril formation, and it has a greater impact than the hexamer-dissociation step. Previous biophysical and biochemical studies showed that the central hydrophobic core region of the B chain (containing residues B11-B17) was the

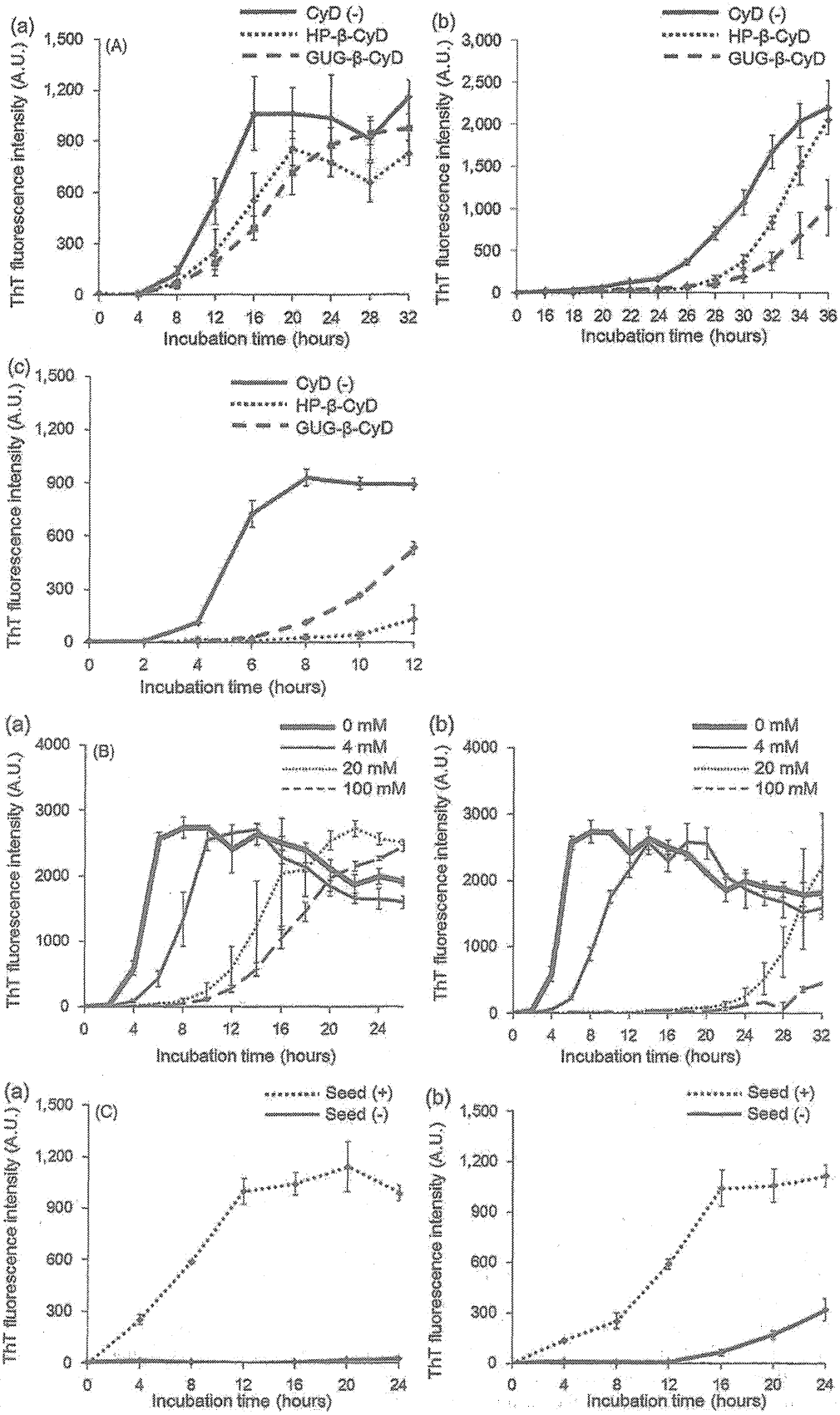

Figure 3. Effects of CyDs on insulin amyloid fibril formation. A, The time course of formation of amyloid fibrils derived from (a) human insulin, (b) insulin aspart, and (c) insulin detemir. Solid lines: without CyDs. Dotted lines: with HP-β-CyD. Dashed lines: with GUG-β-CyD. B, Concentration-dependent inhibitory effects of (a) GUG-β-CyD and (b) HP-β-CyD on amyloid fibril formation of insulin detemir. C, Kinetics of amyloid fibril formation of insulin aspart with (a) GUG-β-CyD and (b) HP-β-CyD. Dotted lines: with 1% of preformed amyloid seeds. Solid lines: without 1% of preformed amyloid seeds. A.U., arbitrary unit.

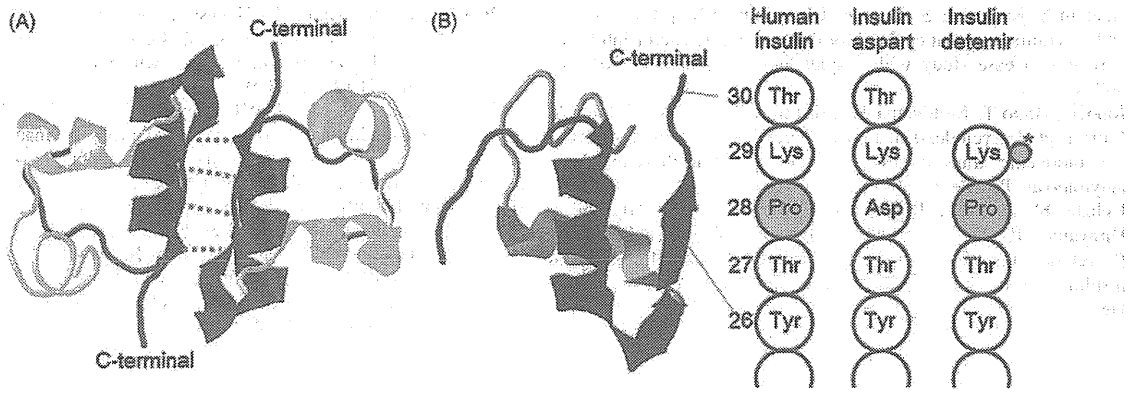

Figure 4. Structure of the C-terminal domain of the insulin B chain A, dimeric form of human insulin (PDB code: 4AK0). Gray and black chains depict insulin A and B chain, respectively. Dotted lines indicate the hydrogen bonds in the C-terminal residues of the B chains. B, Human insulin monomer (PCB code: 3E7Y). Amino acid modifications in the C-terminal domain of the insulin B chain in aspart and detemir. Gray filled and open amino acids indicate hydrophobic and hydrophilic residues, respectively. Asterisk indicates addition of myristic fatty acid (a hydrophobic modification) to lysine.

main contributor to nuclear formation and assembly into amyloid fibrils [14]. Our results suggest that the C-terminus of the B chain also has an important role in nuclear formation, probably by modifying the surface exposure of the hydrophobic core region of the B chain. Previous studies of lysozyme, basic fibroblast growth factor, transthyretin, and insulin reported that β-CyDs interacted with hydrophobic amino acids on the protein surface and stabilized the native structure [22,23]. The hydrophobic cavity of β-CyDs may include the hydrophobic amino acids of insulin and insulin analogues, which may result in the prevention amyloid fibril formation. Substitution of a hydrophobic proline with a hydrophilic aspartic acid in aspart and deletion of a hydrophilic threonine in detemir alters the hydrophobicity of the B chain C-terminus, and may influence their amyloidogenicity and interaction with hydrophobic cavity of CyDs (Figure 4). Because each CyD has a different affinity for complexation with the proteins, the different inhibitory effect on insulin amyloid fibril formation as shown in Figure 3(A) is probably due to the different affinities of the different CyDs for human insulin and insulin analogues.

Because of their low toxicity, CyD derivatives are utilized in the pharmaceutical field at the concentration used in the present study [16]. Also, Jono et al. demonstrated that GUG-β-CyD inhibited TTR aggregation with no toxic effect in a transgenic rat model [18].

In summary, our studies of the amyloid fibril formation kinetics of human insulin and insulin analogues demonstrated that the C-terminal domain of the insulin B chain, in addition to the stability of the insulin dimers and hexamer, had an important role in amyloid fibril formation. In addition, the inhibitory effect of CyDs on insulin amyloid fibril formation may be applicable to the prevention of subcutaneous insulin balls.

Declaration of interest

The authors declare no conflict of interest.

References

1. Sipe JD, Benson MD, Buxbaum JN, Ikeda S, Merlini G, Saraiva MJ, Westermark P. Nomenclature 2014: amyloid fibril proteins and clinical classification of the amyloidosis. Amyloid 2014;21:221–4.
2. Pickup JC. Amyloid and insulin infusion pumps. Diabet Med 1985; 2:13–16.
3. Dische FE, Wernstedt C, Westermark GT, Westermark P, Pepys MB, Rennie JA, Gilbey SG, et al. Insulin as an amyloid-fibril protein at sites of repeated insulin injections in a diabetic patient. Diabetologia 1988;31:158–61.
4. Swift B. Examination of insulin injection sites: an unexpected finding of localized amyloidosis. Diabet Med 2002;19:881–2.
5. Lonsdale-Eccles AA, Gonda P, Gilbertson JA, Haworth AE. Localized cutaneous amyloid at an insulin injection site. Clin Exp Dermatol 2009;34:e1027–8.
6. Nagase T, Katsura Y, Iwaki Y, Nemoto K, Sekine H, Miwa K, Oh-I T, et al. The insulin ball. Lancet 2009;373:184. doi: 10.1016/S0140-6736(09)60041-6.
7. Yumlu S, Barany R, Eriksson M, Röcken C. Localized insulin-derived amyloidosis in patients with diabetes mellitus: a case report. Hum Pathol 2009;40:1655–60.
8. Sie MP, van der Wiel HE, Smedts FM, de Boer AC. Human recombinant insulin and amyloidosis: an unexpected association. Neth J Med 2010;68:138–40.
9. Kudo-Watanuki S, Kurihara E, Yamamoto K, Mukai K, Chen KR. Coexistence of insulin-derived amyloidosis and an overlying acanthosis nigricans-like lesion at the site of insulin injection. Clin Exp Dermatol 2013;38:25–9.
10. Shikama Y, Kitazawa J, Yagihashi N, Uehara O, Murata Y, Yajima N, Wada R, et al. Localized amyloidosis at the site of repeated insulin injection in a diabetic patient. Intern Med 2010;49:397–401.
11. Sheldon B, Russell-Jones D, Wright J. Insulin analogues: an example of applied medical science. Diabetes Obes Metab 2009;11: 5–19.
12. Burke MJ, Rougvie MA. Cross-protein structures. I. Insulin fibrils. Biochemistry 1972;11:2435–9.
13. Bouchard M, Zurdo J, Nettleton EJ, Dobson CM, Robinson CV. Formation of insulin amyloid fibrils followed by FTIR simultaneously with CD and electron microscopy. Protein Sci 2000;9: 1960–7.
14. Ivanova MI, Sievers SA, Sawaya MR, Wall JS, Eisenberg D. Molecular basis for insulin fibril assembly. Proc Natl Acad Sci USA 2009;106:18990–5.
15. Nayak A, Dutta AK, Belfort G. Surface-enhanced nucleation of insulin amyloid fibrillation. Biochem Biophys Res Commun 2008; 369:303–7.
16. Crini G. Review: a history of cyclodextrins. Chem Rev 2014;114: 10940–75.

17. Gautam S, Karmakar S, Bose A, Chowdhury PK. β-Cyclodextrin and curcumin, a potent cocktail for disaggregating and/or inhibiting amyloids: a case study with α-synuclein. Biochemistry 2014;53: 4081–3.
18. Jono H, Anno T, Motoyama K, Misumi Y, Tasaki M, Oshima T, Mori Y, et al. Cyclodextrin, a novel therapeutic tool for suppressing amyloidogenic transthyretin misfolding in transthyretin-related amyloidosis. Biochem J 2011;437:35–42.
19. Uehata K, Anno T, Hayashida K, Motoyama K, Higashi T, Hirayama F, Ono N, et al. Effects of selected anionic β-cyclodextrins on persistence of blood glucose lowering by insulin glargine after subcutaneous injection to rats. J Drug Deliv 2011;2011:195146. doi:10.1155/2011/195146.
20. Uehata K, Anno T, Hayashida K, Higashi T, Motoyama K, Hirayama F, Uekama K, et al. Peak-less hypoglycemic effect of insulin glargine by complexation with maltosyl-β-cyclodextrin. Int J Pharm 2012;422:33–9.
21. Surmacz-Chwedoruk W1, Nieznańska H, Wójcik S, Dzwolak W. Cross-seeding of fibrils from two types of insulin induces new amyloid strains. Biochemistry 2012;51:9460–9.
22. Tavornvipas S, Tajiri S, Hirayama F, Arima H, Uekama K. Effects of hydrophilic cyclodextrins on aggregation of recombinant human growth hormone. Pharm Res 2004;21:2369–76.
23. Tavornvipas S, Hirayama F, Takeda S, Arima H, Uekama K. Effects of cyclodextrins on chemically and thermally induced unfolding and aggregation of lysozyme and basic fibroblast growth factor. J Pharm Sci 2006;95:2722–9.

Liver Transplantation for Hereditary Transthyretin Amyloidosis: After 20 Years Still the Best Therapeutic Alternative?

Bo-Göran Ericzon,[1] Henryk E. Wilczek,[1] Marie Larsson,[1] Priyantha Wijayatunga,[2] Arie Stangou,[3] João Rodrigues Pena,[4] Emanuel Furtado,[5] Eduardo Barroso,[4] Jorge Daniel,[6] Didier Samuel,[7] Rene Adam,[7] Vincent Karam,[7] John Poterucha,[8] David Lewis,[9] Ben-Hur Ferraz-Neto,[10] Márcia Waddington Cruz,[11] Miguel Munar-Ques,[12] Juan Fabregat,[13] Shu-ichi Ikeda,[14] Yukio Ando,[15] Nigel Heaton,[16] Gerd Otto,[17] and Ole Suhr[18]

Background. Until recently, liver transplantation (Ltx) was the only available treatment for hereditary transthyretin (TTR) amyloidosis; today, however, several pharmacotherapies are tested. Herein, we present survival data from the largest available database on transplanted hereditary TTR patients to serve as a base for comparison. **Methods.** Liver transplantation was evaluated in a 20-year retrospective analysis of the Familial Amyloidosis Polyneuropathy World Transplant Registry. **Results.** From April 1990 until December 2010, data were accumulated from 77 liver transplant centers. The Registry contains 1940 patients, and 1379 are alive. Eighty-eight Ltx were performed in combination with a heart and/or kidney transplantation. Overall, 20-year survival after Ltx was 55.3%. Multivariate analysis revealed modified body mass index, early onset of disease (<50 years of age), disease duration before Ltx, and TTR) Val30Met versus non-TTR Val30Met mutations as independent significant survival factors. Early-onset patients had an expected mortality rate of 38% that of the late-onset group ($P < 0.001$). Furthermore, Val30Met patients had an expected mortality rate of 61% that of non-TTR Val30Met patients ($P < 0.001$). With each year of duration of disease before Ltx, expected mortality increased by 11% ($P < 0.001$). With each 100-unit increase in modified body mass index at Ltx, the expected mortality decreased to 89% of the expected mortality ($P < 0.001$). Cardiovascular death was markedly more common than that observed in patients undergoing Ltx for end-stage liver disease. **Conclusions.** Long-term survival after Ltx, especially for early-onset TTR Val30Met patients, is excellent. The risk of delaying Ltx by testing alternative treatments, especially in early-onset TTR Val30Met patients, requires consideration.

(*Transplantation* 2015;00: 00–00)

The first report of the outcome of liver transplantation (Ltx) for hereditary transthyretin (h-TTR) amyloidosis, previously designated familial amyloid polyneuropathy (FAP), was published in 1993 in the Lancet,[1] and it described the outcome for 4 patients with the TTR Val30Met mutation who had been followed up for 1 to 2 years after the procedure. The impression was that the procedure was successful,

Received 30 October 2014. Revision requested 7 July 2014.

Accepted 30 September 2014.

[1] *Division of Transplantation Surgery, Karolinska University Hospital Huddinge, Stockholm, Sweden.*

[2] *Department of Statistics, Umeå University, Umeå, Sweden.*

[3] *Liver Unit, Queen Elizabeth Hospital, Birmingham, United Kingdom.*

[4] *Liver Transplant Unit, Hospital de Curry Cabral, Lisbon, Portugal.*

[5] *Unidade de Transplantação Hepática Pediátrica e de Adultos, Centro Hospitalar e Universitário de Coimbra, Portugal.*

[6] *Liver Transplant Unit, Hospital de Santo António, Porto, Portugal.*

[7] *AP-HP, Hôpital Paul Brousse, Centre Hépatobiliaire, Univ Paris-Sud, Villejuif, France.*

[8] *Liver Transplant/Gastroenterology, Mayo Clinic College of Medicine, Rochester, MN.*

[9] *Hepatobiliary Surgery and Liver Transplantation, Lahey Medical Center, Burlington, MA.*

[10] *Department of Liver Transplantation, Hospital Israelita Albert Einstein, Sao Paulo, Brazil.*

[11] *Department of Neurology, Federal University of Rio de Janeiro, Rio de Janeiro, Brazil.*

[12] *Grupo de Estudio de la PAF, Palma de Mallorca, Spain.*

[13] *Liver Transplant Unit, University Hospital Bellvitge, Spain.*

[14] *Third Department of Medicine, Shinshu University School of Medicine, Matsumoto, Japan.*

[15] *Department of Neurology, Graduate School of Medical Science Kumamoto University, Kumamoto, Japan.*

[16] *Liver Unit, King's College Hospital, London, United Kingdom.*

[17] *Klinik für Allgemein-, Viszeral- und Transplantationschirurgie, J Gutenberg-Universität, Mainz, Germany.*

[18] *Department of Public Health and Clinical Medicine, Umeå University Hospital, Umeå, Sweden.*

The authors declare no conflicts of interest.

Financial support: Karolinska University Hospital, Karolinska Institutet, Astellas Pharma Great Britain, and Sandoz Nordic AS are sponsors of FAPWTR.

The funding sources had no involvement in the collection, analysis, and interpretation of data, in the writing of the article, or in the decision to submit the article for publication.

B.G.E., H.E.W., and O.S. initiated the working hypothesis and participated in the research design, performance of the research and data acquisition, the analysis and interpretation of data and writing of the article. M.L. maintained contact with the study centers, assembled and validated the data for analysis and participated in the writing of the report. P.W. performed data and statistical analysis and participated in the analysis and interpretation of data and commented on drafts of the report. A.S., J.R.P., E. F., E.B., J.D., D.S., R.A., V.K., J.P., D.L., B.H.F.N., M.W.C., M.M.Q., J.F., S.I.I., Y.A., N. H., and G.O. contributed by revising the manuscript and giving valuable input on the content and design. All authors were active in reviewing and finalizing the article.

Correspondence: Bo-Göran Ericzon, MD, PhD, Division of Transplantation Surgery, F82, Karolinska University Hospital Huddinge, SE-14186 Stockholm, Sweden. (bo-goran.ericzon@ki.se)

ISSN: 0041-1337/15/0000-00

DOI: 10.1097/TP.0000000000000574

with symptomatic improvement for some patients, and that a regression of the amyloid load, measured by serum amyloid protein scintigraphy, could be observed. This was a major achievement against this previously intractable fatal systemic amyloid disease. However, subsequent analysis over the following years disclosed less favorable outcomes for those carrying non-TTR Val30Met mutations[2-4] and also for malnourished patients and those with longstanding and advanced disease.[5-7] Differences between patients with early onset compared to those with late onset of the disease were observed.[8] Heart complications after transplantation were the dominant problem.[2-4,9,10] It is obvious that careful selection of patients is necessary to achieve acceptable outcomes.

The Familial Amyloidotic Polyneuropathy World Transplant Registry (FAPWTR) was established in 1995 by a group of investigators taking part in the First International Workshop on Liver Transplantation for Familial Amyloidotic Polyneuropathy, held at Karolinska Institutet in Stockholm, Sweden in 1993. The purpose was to monitor international experience with Ltx for this indication and to promote collaboration and ultimately improve patient selection and results. The registry now contains accumulated survival data from more than 20 years of follow-up of transplanted h-TTR amyloidosis patients from 1990 onward. These data are now of vital importance, with the arrival of medical therapy for the disease. The first compound, tafamidis, is a stabilizing agent that helps to prevent the tetrameric TTRs from dissociating into monomers and assembling into amyloid fibrils.[11] However, several other treatment modalities, including silencing RNA,[12] and diflunisal,[13] are going into clinical trials. Tafamidis demonstrated efficacy in slowing down the progression rate of the disease in a controlled trial,[14] and it is now approved by the European Medical Agency for treatment of h-TTR amyloidosis at early stages of the disease. However, its efficacy for long-term treatment has not been assessed, and the cost appears to be substantially higher than that of Ltx. Recently, it was suggested that patients with early-stage h-TTR amyloidosis should initially be treated by tafamidis, and if their disease progressed, they should be considered for Ltx.[15] However, this strategy is questionable because the patient would be in a less favorable position for transplantation with more-advanced disease.

The efficacy of new treatments should principally be compared with currently available treatment modalities. It appears to be impossible to carry out a comparative study between Ltx, which is the currently accepted treatment for h-TTR, and the new medical treatment, tafamidis. However, Ltx remains the gold standard against which new treatments should be measured, and the long-term outcome for Ltx patients can be assessed from the data in FAPWTR. The aim of the present study was to evaluate the mortality of h-TTR amyloidosis patients who underwent Ltx, based on data in the FAPWTR collected over the course of 20 years.

MATERIALS AND METHODS

Seventy-seven centers in 19 countries report data related to Ltx for TTR amyloidosis to the FAPWTR. An initial report is given at the time of Ltx. In addition, retransplantation, patient death, or loss to follow-up, as well as if an additional organ transplantation is performed, such as heart or kidney combinations with a Ltx, are also reported. Participating centers are requested to provide annual follow-up data on patients who were previously reported to the register. Information regarding demographics, heredity, type of TTR mutation, clinical manifestations, and peripheral and autonomic neuropathy are recorded. Patient weight, height, and serum albumin are recorded for calculation of the modified body mass index (mBMI). The pretransplant value of this index has been reported to correlate with the prognosis after transplantation.[18] The index is calculated by multiplying the BMI of the patient by the level of serum albumin; thus, there is compensation for the presence of oedema in malnourished patients, which may yield a falsely high BMI.

Results from the FAPWTR are reported back to collaborating members on a yearly basis. The FAPWTR data are also to some extent shown on its homepage (www.fapwtr.org). It is also possible to download report forms from the homepage.

In the present analysis, patients who were reported to FAPWTR until December 2010, with a minimum follow-up of 1 year, were included. Patients not reported as dead and with no follow-up after January 1, 2010 were regarded as lost to follow-up.

Statistical Analysis

To test for differences between means of normally distributed data from different patient categories, Student *t* test was used. Patient survival probabilities were calculated by Kaplan-Meier estimation. The log-rank test (Mantel Cox) was used to test the equality of survival patterns among different categories of patients. All statistical tests were 2-sided and conducted at the 0.05 significance level. Unless stated otherwise, statistics are presented as mean ± standard deviation. Univariable analysis was performed using the logistic regression model and significant variables were put into the Cox multivariate proportional hazards model to determine the risk factors associated with survival. The assumptions of proportional hazards were checked by analyzing plots of the log cumulative hazard stratified by factors used in the model and by analyzing plots of Schoenfeld residuals versus survival time. Variables were added stepwise to the model, selecting the most statistically significant variable first. Then an analysis was done to find the following variable that, together with the first variable, best prognosticated survival. Variables were added until no improvement in prediction was seen as assessed by an increase in the log-likelihood value. Finally, findings based on stepwise addition were confirmed by a stepwise deletion. This was done by forcing all variables into the model after which variables were successively eliminated, based on which of the remaining variables delivered the smallest reduction in the log-likelihood value. Odds ratios and hazard ratios with their *P* values were estimated between different groups and reported in Table 2. Covariates were tested for independence, and no significant multicolinearity was identified for the covariates.

RESULTS

Approximately 125 liver transplants were performed and reported yearly worldwide for h-TTR amyloidosis, with a potential reduction in transplantation activity over the last 2 years (Figure 1). A total of 1940 patients underwent 2127 Ltxs, and 561 patient deaths were reported to the registry. One hundred and eighty-eight retransplantations were